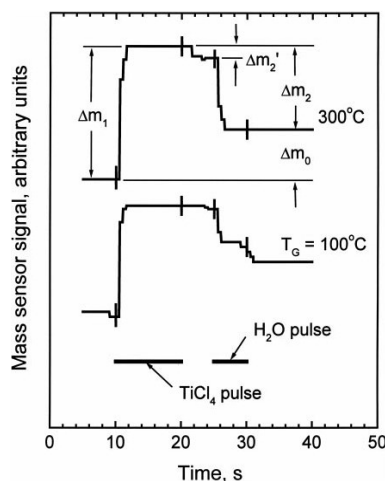


## Electronic Supplementary Information

### Mesoporous TiO<sub>2</sub> Anatase Films for Enhanced Photocatalytic Activity under UV and Visible Light

Olga M. Ishchenko<sup>\*a, b, f</sup>, Guillaume Lamblin,<sup>a</sup> Jérôme Guillot,<sup>a</sup> Ingrid C. Infante,<sup>c</sup> Maël Guennou,<sup>d</sup> Nouredine Adjeroud,<sup>a</sup> Ioana Fechete,<sup>b, g, h</sup> Francois Garin,<sup>b</sup> Philippe Turek,<sup>e</sup> Damien Lenoble<sup>\*a</sup>



**Figure S1.** Schematic illustration of mass evolution during an ideal ALD deposition from TiCl<sub>4</sub> and water. Reproduced from Aarik et al.<sup>29</sup>

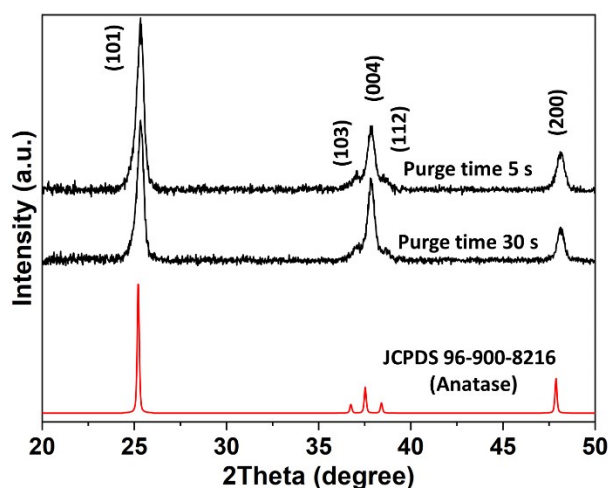


**Figure S2.** X-ray diffraction data of the annealed TiO<sub>2</sub> samples deposited at room temperature using different purges times (5 s and 30 s). Reference anatase spectra (JCPDS sheet indicated).

Figures S3 and S4 presented bellow to illustrate the films morphology modification before and after the thermal annealing process. The amorphous films present flat contrast characteristic of a homogeneous film (Fig. S3) while after the annealing we note in the film the clear formation of a mesoporous structure with a different topography and granular structure (Fig. S4).

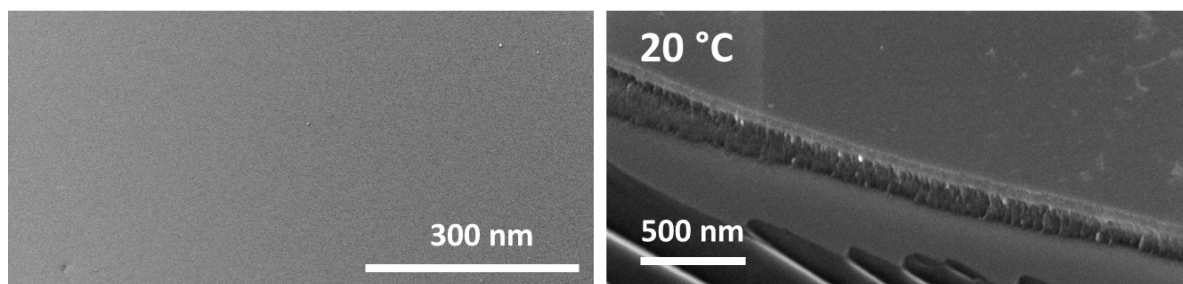


**Figure S3.** SEM images of amorphous film deposited at RT: (left) top view, and (right) tilted view.

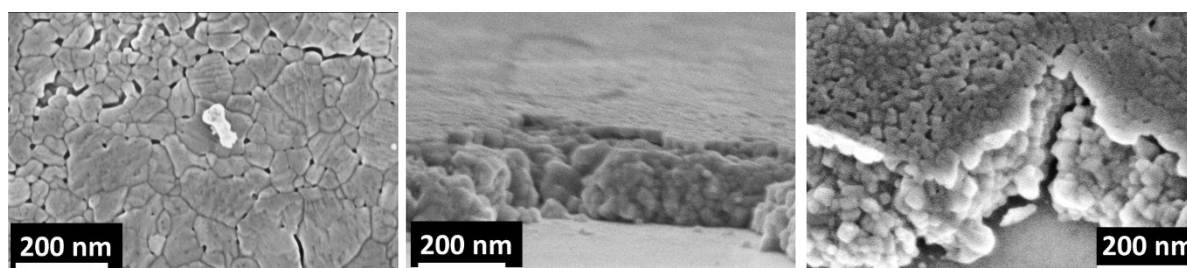


**Figure S4.** SEM images of RT TiO<sub>2</sub> film deposited in short purge time regime: (left) top view, and (centre and right) tilted views.

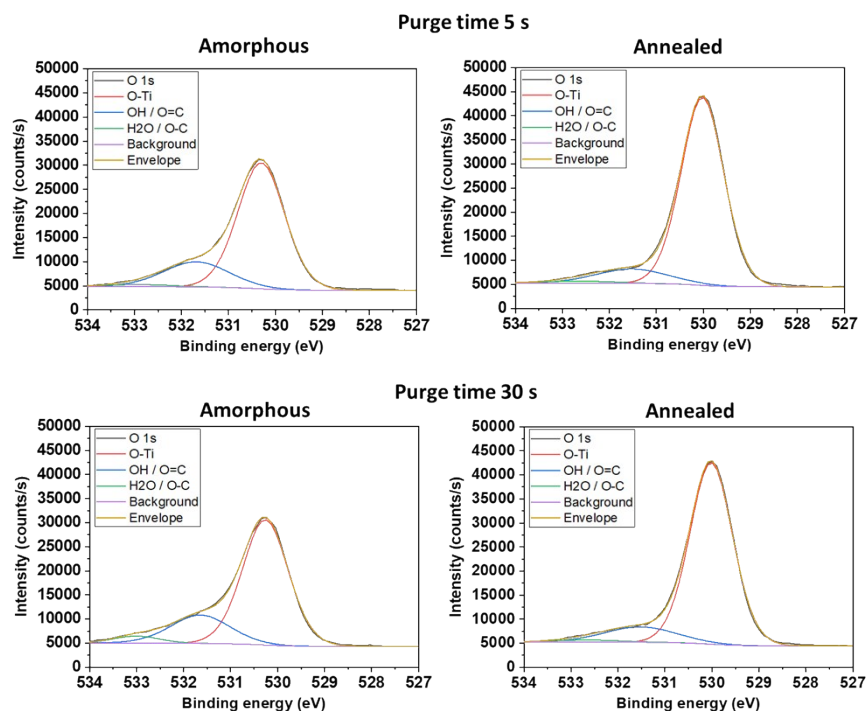


**Figure S5.** XPS O 1s spectra from the surface of amorphous and annealed samples, grown in short (5 s) and long (30 s) purge time regimes.

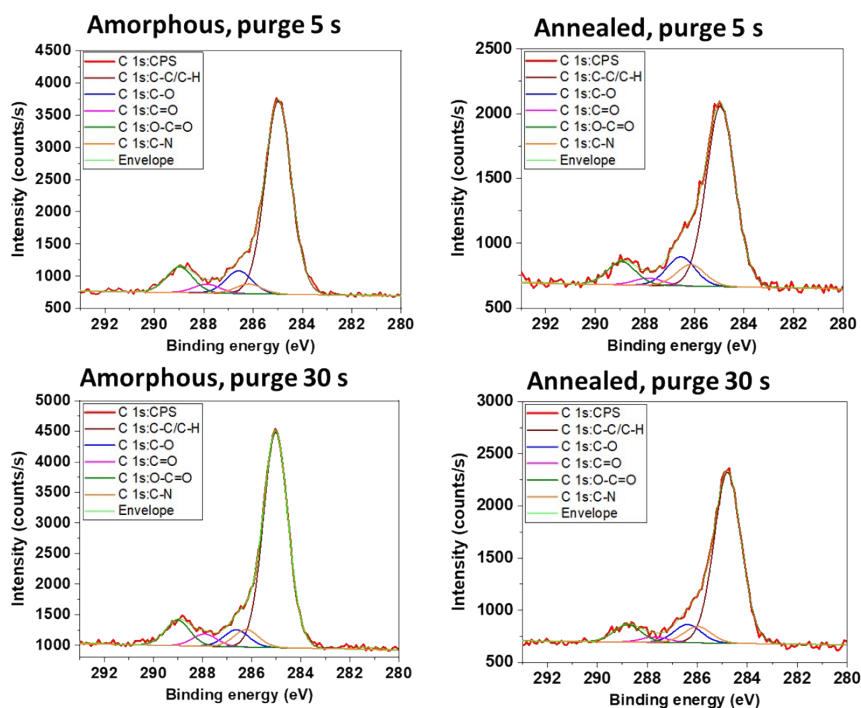


**Figure S6.** XPS C 1s spectra from the surface of amorphous and annealed samples, grown in short (5 s) and long (30 s) purge time regimes.

The oxygen contribution related to titanium (O-Ti) was determined by subtracting from the total oxygen contribution the oxygen contribution for SiO<sub>2</sub> and all detected oxygen contributions related to carbon:

$$[O - Ti] = [O1s] - 2 \times [Si2p] \times \frac{[SiO_2]}{100} - [C1s] \times \frac{[C - O] + [C = O] + 2 \times [O - C = O]}{100}$$

**Table S1.** Elemental composition of samples deposited at RT after 965 cycles, purge time of 5 and 30 s, before and after annealing, at.%.

		As deposited		Annealed		
		Surface	Volume	Surface	Volume	
<b>Purge 5 s</b>	<b>Elemental composition (at.%)</b>	<b>Ti</b>	23	33	27	36
		<b>O</b>	53	63	60	65
		<b>C</b>	21	0	11	0
		<b>Cl</b>	1	2→6*	0	0
		<b>N</b>	1	0	0	0
		<b>Si</b>	1	0	2	0
<b>Purge 30 s</b>	<b>Elemental composition (at.%)</b>	<b>Ti</b>	21	34	26	35
		<b>O</b>	51	63	60	65
		<b>C</b>	22	0	11	0
		<b>Cl</b>	4	4	0	0
		<b>N</b>	1	0	0	0
		<b>Si</b>	1	0	3	0

\*Presence of Cl increases with the depth

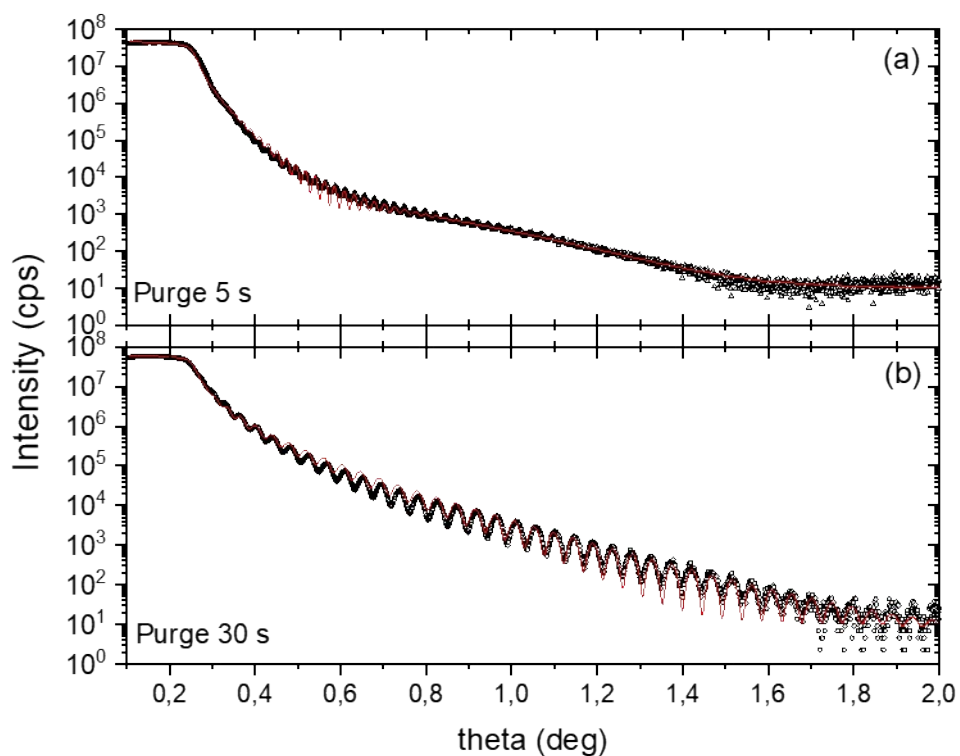


**Figure S7.** X-ray reflectometry data (symbols) and corresponding fits (lines) obtained using X'Pert Reflectivity (PANalytical B.V.) software on TiO<sub>2</sub> films on Si under purge of (a) 5 s and (b) 30 s. Theta corresponds to the incident angle.

**Table S2.** X-ray reflectometry fitting results, including the TiO<sub>2</sub> layer density and corresponding thickness and associated films surface and mass values used in the photocatalytic measurements. A 0.7-1 nm SiO<sub>2</sub> layer was used as top Si-substrate surface, at the interface with TiO<sub>2</sub> layers.

TiO <sub>2</sub> films deposition regimes	Density, g/cm <sup>3</sup>	Thickness, nm	Sample surface, cm <sup>2</sup>	Mass, g
Purge 5 s on Si	3.39	2.67	2.06	1.13·10 <sup>-4</sup>
	3.18	169.9		
Purge 30 s on Si	3.16	93.13	2.99	8.80·10 <sup>-5</sup>

## Photocatalytic measurement for samples deposited on Si/SiO<sub>2</sub> substrates

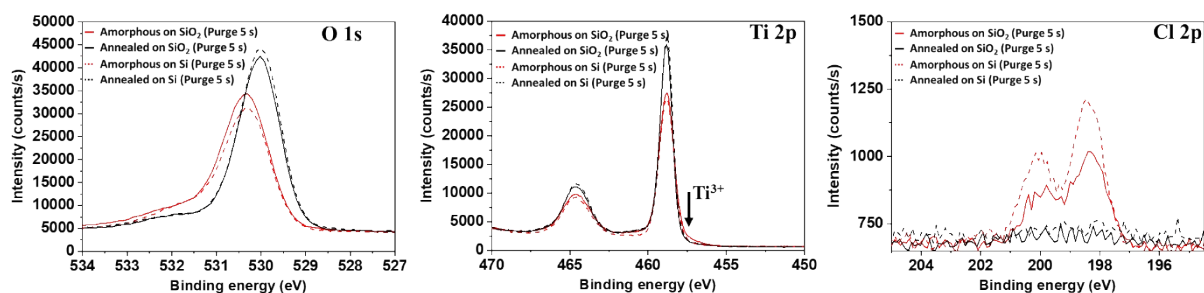


**Figure S8.** XPS O 1s (left panel), Ti 2p (center panel) and Cl 2p (right panel) spectra on surface of amorphous and annealed samples, grown in short (5 s) on Si and Si/SiO<sub>2</sub> substrates.

The investigation of the photocatalytic activity of samples deposited in the short purge time regime (5 s) on the thermally oxidized 40 nm SiO<sub>2</sub> layer (Si/SiO<sub>2</sub>) under both UV and visible ranges irradiation reveals a significant improvement of the photocatalytic degradation rate for the TiO<sub>2</sub> thin films (Figure S9).

From the Ti 2p<sub>3/2</sub> surface spectra (Figure S8), we observe a slight contribution of Ti<sup>3+</sup> at 457.0 eV in the annealed TiO<sub>2</sub> film deposited on Si/SiO<sub>2</sub> substrate that could be the reason for the improved photocatalytic activity.

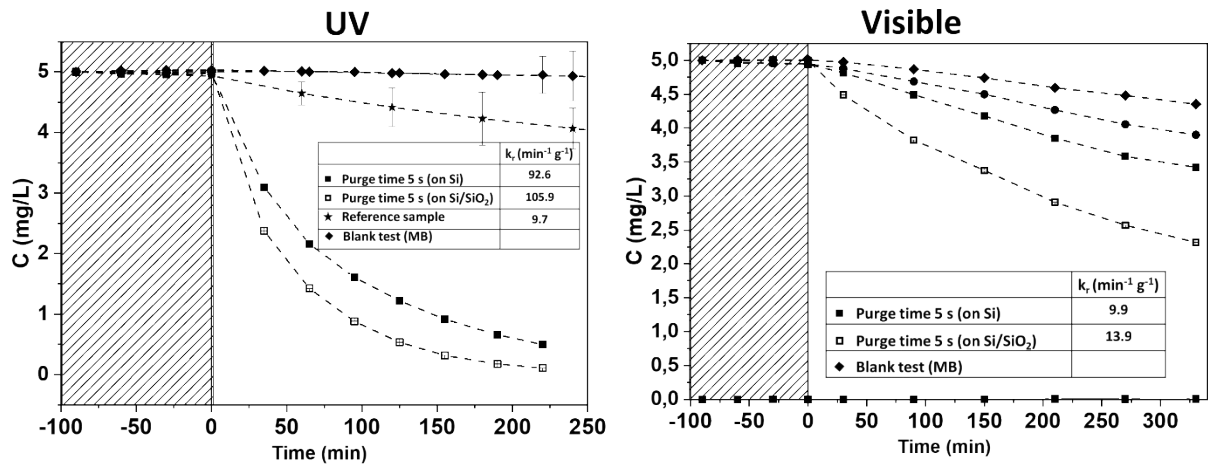


**Figure S9.** Photocatalytic degradation of MB in UV and visible range on TiO<sub>2</sub> films grown in short purge time regime (5 s) on Si(100) with native silicon oxide and thermally oxidized 40 nm silica layer SiO<sub>2</sub>/Si; insert table of the photocatalytic degradation constant normalised by the TiO<sub>2</sub> mass.

In order to calculate the photocatalytic degradation constant ( $k_r$ ) per mass unit, we measured the film thickness and density by X-ray reflectometry measurements (Figure S7 and Table S2). That allowed us to determine the mass of the deposited TiO<sub>2</sub> (after annealing) and proceed further constants normalization.

**Table S3.** Photocatalytic degradation constants  $k_r$  of TiO<sub>2</sub> films deposited at RT in the UV range.

TiO <sub>2</sub> films deposition regimes	Photocatalytic degradation constant, $\times 10^{-3} \text{ min}^{-1}$		Photocatalytic degradation constant, normalized by surface unit, $\times 10^{-4} \text{ min}^{-1} \text{ cm}^{-2}$		Photocatalytic degradation constant, normalized by mass unit, $\text{min}^{-1} \text{ g}^{-1}$	
	On Si	On Si/SiO <sub>2</sub>	On Si	On Si/SiO <sub>2</sub>	On Si	On Si/SiO <sub>2</sub>
Purge 5 s (170 nm)	10.5	17.2	50.9	57.6	92.6	105.9
Purge 30 s (90 nm)	4.7	5.7	15.7	19	53.4	64.5
Reference sample (90 nm)	0.8	-	2.8	-	9.7	

In the UV range we note the higher degradation rate for the sample deposited on the on Si/ SiO<sub>2</sub> sample. The photocatalytic degradation constant normalized by the TiO<sub>2</sub> mass unit was 105.9 min<sup>-1</sup> g<sup>-1</sup> on Si/SiO<sub>2</sub> contrary to 92.6 min<sup>-1</sup> g<sup>-1</sup> on Si (100) substrate with native silica (Figure S9).

In the visible range, the MB has natural photodegradation, however we also note a similar improvement tendency for the photocatalytic degradation constant normalized by the TiO<sub>2</sub> mass, we found a value of 13.9 min<sup>-1</sup> g<sup>-1</sup> for mesoporous TiO<sub>2</sub> deposited on the thermal silica layer, and 9.9 min<sup>-1</sup> g<sup>-1</sup> in case of the silicon substrate with native silica (Figure S9).

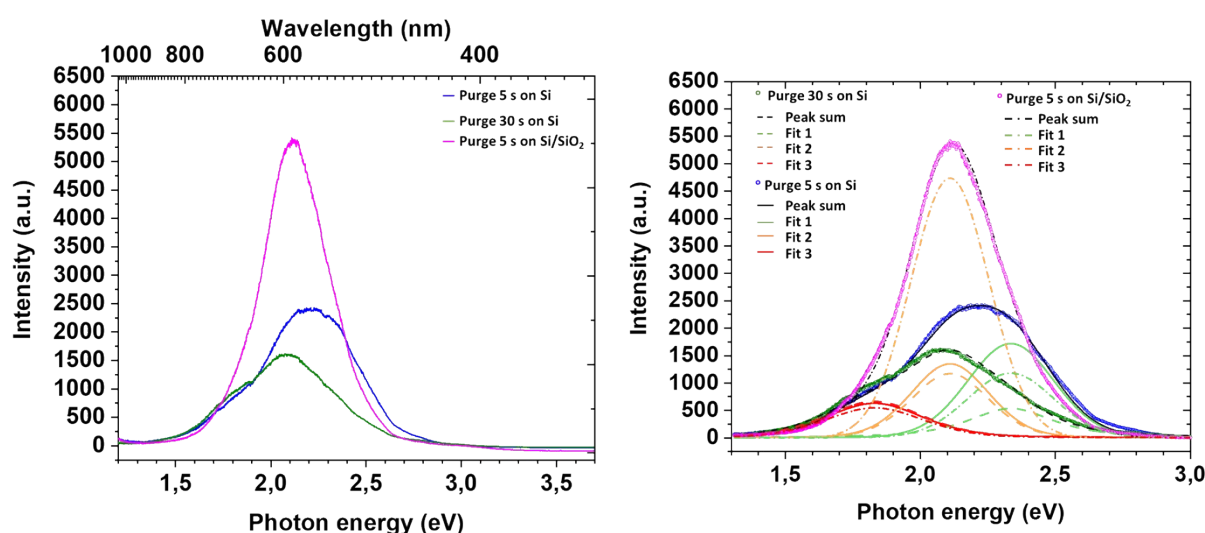


**Figure S10.** PL spectra of mesoporous TiO<sub>2</sub> films deposited on Si and Si/SiO<sub>2</sub> substrates and their deconvolution.

### Surface saturation tests

The mesoporous samples usually present a high surface area value, therefore the MB adsorption on the surface (i.e., without any degradation) should be checked. To this end the samples were kept in MB solution in the dark for up to 18 h and did not show any change in MB concentration. Further, to determine the photocatalyst surface saturation with adsorbed and non-degraded



pollutant molecules, cyclic photocatalytic measurements were performed on the same sample up to 4 degradation runs (Figure S11). The photocatalytic degradation rate was unchanged even after 4 runs, that is highlighting the very high stability and efficacy of our samples. After 4 h, the MB is fully degraded, regardless of the number of experiments performed with the same sample.

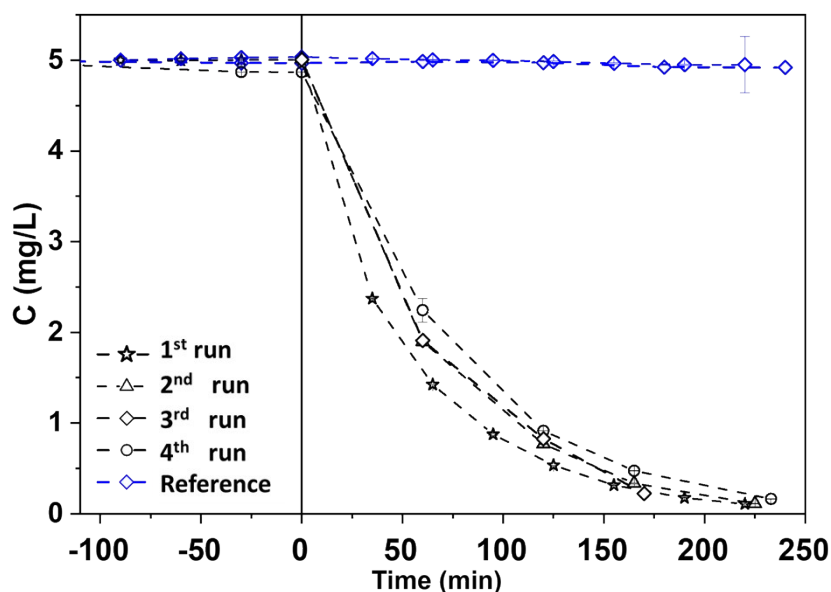


**Figure S11.** Repeatability of the MB photocatalytic degradation in the UV range (4 cyclic measurements)

### Repeatability

The reproducibility of the proposed photocatalytic systems was verified for films deposited on Si/SiO<sub>2</sub> substrates. Two series of samples were deposited in the same ALD experimental conditions except the reactor pressure was varied from 3.5 mbar (series 1) to 2.5 mbar (series 2) due to the freshly performed pump maintenance. In the configuration of the ALD reactor, the pump extraction flow cannot be controlled by a valve. The comparison between these two series confirmed the highlighted efficiency of the photocatalytic degradation. However, the

degradation rate was lower in the case of the second deposition series (Figure S12). Unfortunately, it was impossible to establish exactly the same pressure conditions due to technical limitations.

In view of these results, we plan to investigate the photocatalytic performance of new films grown under different pressures, after technical changes in the ALD chamber are done to allow accurately handling the working ALD chamber pressure.

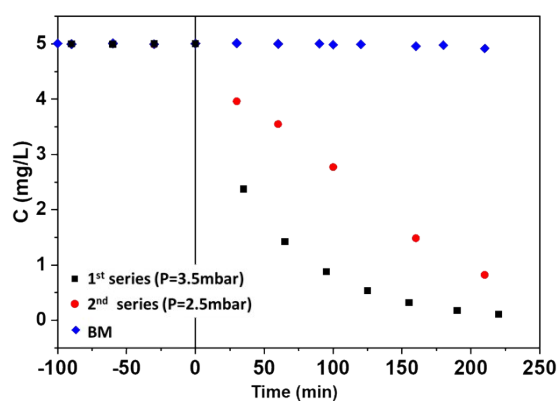


**Figure S12.** Photocatalytic degradation of MB in UV range on TiO<sub>2</sub> films of series 1 and 2, deposited on Si/SiO<sub>2</sub> substrates.